Alma Mater Studiorum Università di Bologna
Archivio istituzionale della ricerca

Silicon(IV) Corroles

(Article begins on next page)

20 April 2024

Silicon (IV) corroles.

Giuseppe Pomarico,[a] Donato Monti,[a] Martina Bischetti,[a] Andrea Savoldelli,[a] Frank R. Fronczek,[b] Kevin M. Smith,[b] Damiano Genovese,[c] Luca Prodi,[c] and Roberto Paolesse*[a]

Dedicated to Professor Giuseppe Palleschi on the occasion of his 70th birthday

Abstract: Silicon complexes of corrole have been obtained for the first time by reaction of the corrole free-base with hexachlorodisilane. The peripheral substituents of corrole strongly influence the nature of the reaction products: β-octaalkylcorrole has been mainly isolated as the μ-oxo dimer, while a hydroxo-complex is obtained in the case of the 5,10,15-tris-(pentafluorophenyl)corrole. In the case of *meso*-tritolylcorrole, a mixture of monomer/μ-oxo dimer is obtained. The silicon-corrole complexes are more stable toward hydrolysis than are the corresponding porphyrin derivatives and are endowed with brilliant luminescence properties. The large affinity of silicon toward fluoride ion allowed an investigation of the ability of this compound to serve as a sensor for F- detection. The strong color variation due to the halide interaction makes the Si-corrole an interesting material for the naked-eye detection of inorganic fluoride.

Introduction

Corrole was first reported by Johnson and Kay in the 1964,[1] but its chemistry blossomed after 1999, when two different methods for the preparation of this class of macrocycle, starting from commercially available precursors, were reported.[2] However the impressive interest devoted to this macrocycle cannot be only related to its improved synthetic accessibility, but also to the group of properties that gives to corrole a peculiar role with respect to the more famous porphyrin or phthalocyanine macrocycles.[3] As a ligand, corrole frequently shows so-called non-innocent character,[4] which makes its coordination chemistry unique and interesting for catalytic applications.[5] Corroles are also endowed with brilliant photophysical properties,[6] where either the wavelength and/or the intensity of their absorbance and emission bands can be affected by the coordination of metal ions.

The preparation of corrole derivatives is interesting for the application in several fields of research ranging from solar cells[7] through PDT[8] to optical sensors.[9] In particular, the insertion of the lighter p-block elements allows one to prepare chromophores that can rival the Mg and Zn complexes of tetraphenylporphyrin, which are some of the most fluorescent tetrapyrrolic macrocycles.[10] Examples are the B(III),[11] Al(III),[12] Ga(III),[12b,c,13] Ge(IV)[14] and P(V)[15] derivatives. Quite surprisingly, silicon has not yet been coordinated into the corrole core,[4c,16] although the silicon complex of triaza-tetrabenzcorrole has been obtained by ring contraction of the corresponding silicon phthalocyanine.[17] Optical features of a silicon-corrole should be similar or even better than those of Al(III) or P(V) complexes, considering the small dimension of these p-block ions. We present here a synthetic route for the preparation of silicon complexes of different corroles and the photophysical characterization of these species. Selective binding of fluoride ion has been demonstrated in solution, providing naked ion colorimetric chemosensors for F- detection. This selectivity has been exploited to develop optical sensors for the detection of fluoride ion in water, based on both polymeric membranes or silica-pluronics nanoparticles.

Results and Discussion

Synthesis. The preparation of Si complexes of corrole was first attempted by following the procedure for the preparation of the higher homologues, Ge and Sn corrolates,[14] where a chloride derivative (GeCl$_4$ or SnCl$_2$) is used as the metal ion source and the reaction is performed in refluxing DMF. 5,10,15-Tritolylcorrole free base (TTCorrH$_3$) was dissolved in DMF and an excess of Si$_2$Cl$_6$ was added. The mixture was refluxed for one hour, but the UV-vis spectrum showed only the presence of the corrole cation, probably due to the formation of HCl by Si$_2$Cl$_6$ hydrolysis, which prevented complex formation. We decided to substitute DMF with pyridine, hoping that its more basic character could circumvent this drawback. In this case the solution color turned from green to violet within a few minutes, and no trace of the starting material was detected after one hour. The subsequent work-up yielded two fractions, collected after chromatographic purification. The UV-vis spectrum (Figure 1) of the first band showed a Soret band at 394 nm and some very weak absorbances between 550-600 nm. The mass analysis suggested the formation of the μ-oxo dimeric species **2**, due to the molecular peak at 1203 m/z. The ^{1}H NMR spectrum showed no signals in the negative region, as expected for a

[a] Dr. G. Pomarico, Dr. D. Monti, Ms. M. Bischetti, Dr. A Savoldelli, Prof. R. Paolesse*
Department of Chemical Science and Technologies
University of Rome Tor Vergata
Via della Ricerca Scientifica snc, 00133 Rome, Italy
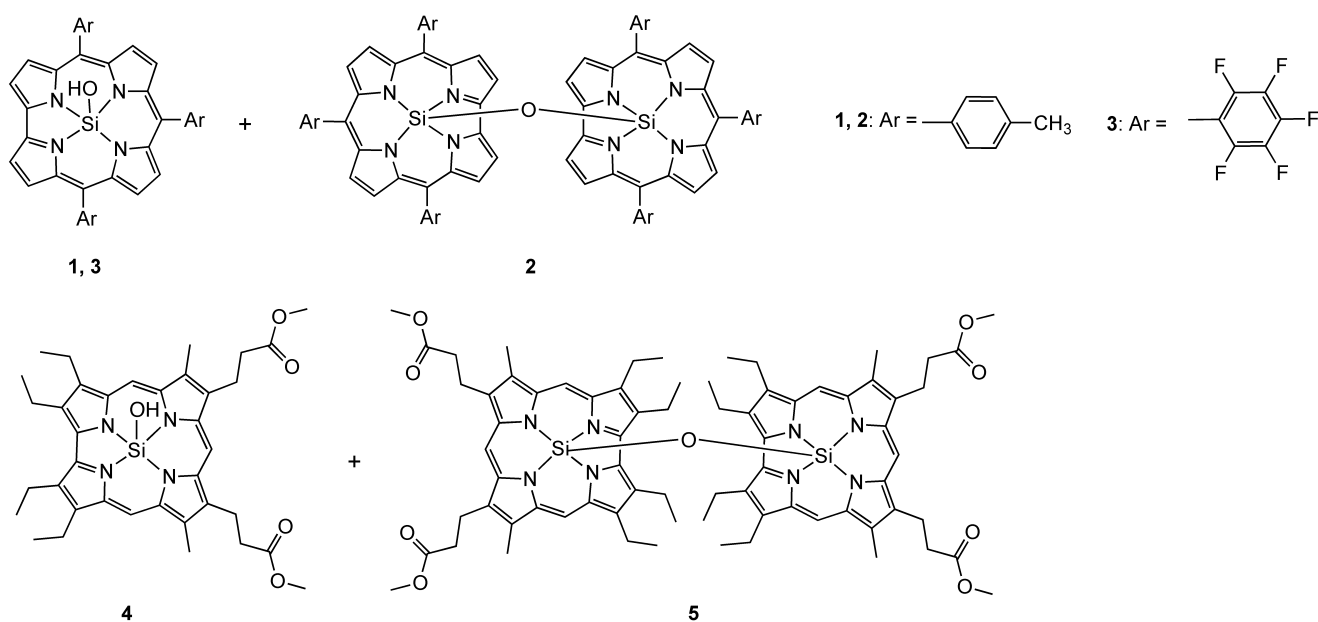E-mail: roberto.paolesse@uniroma2.it
[b] Dr. F. R. Fronczek, Prof. K. M. Smith
Department of Chemistry
Louisiana State University
Baton Rouge, LA, 70803, USA
[c] Dr. D. Genovese, Prof. L. Prodi,
Dipartimento di Chimica "Giacomo Ciamician"
Università di Bologna
via Selmi 2, 40126 Bologna (Italy).

Supporting information for this article are available on the WWW under htpp://dx.doi.org/xxx

Scheme 1. Molecular structures of the silicon corroles investigated

corrole complex without any H-containing axial ligand, while the unresolved signals for the aromatic protons suggested restricted rotation around the Si-O-Si bond. No clear indication about the axial ligand of the Si-corrole complex was obtained from mass analysis for the second most abundant fraction, cherry in color, since the molecular peak corresponds to a molecule of 3-nitrobenzyl alcohol (the FAB matrix) coordinated

Figure 1. UV-vis spectrum of Si(IV)-triarylcorrole **1**, **2**, **3** and **5** in THF solution UV.

to the Si^{4+} ion. The ^{1}H NMR spectrum measured in CDCl$_3$ highlighted the diamagnetic nature of the complex, which presented four sets of doublets for the β-pyrrolic protons in the 8.90-9.36 ppm region, while the –CH$_3$ protons appears as two singlets around 2.70 ppm, with a 1:2 intensity as expected due to the symmetry of the corrole. A broad signal at -4.46 ppm is

related to the axially bound –OH unit. The formation of the Si-corrole was finally confirmed by the X-ray structure shown in Figure 2, which unambiguously identified the structure of the compound as the hydroxo-silicon corrole **1**.

While porphyrin and phthalocyanine complexes of Si(IV) are six-coordinate (81 hits in the Cambridge Structural Database), the smaller corrole enforces a five-coordinate square pyramidal coordination in **1**. The Si atom lies 0.36 Å (average of 3) out of the best plane of the four N atoms. The Si-N distances are within the range 1.838(4) - 1.856(4) Å for the ordered molecule, and its Si-O distance is 1.642(4) Å. The 23-atom corrole core does not deviate greatly from planarity, having mean deviations of 0.039 and 0.074 Å for the two independent molecules.

Corrole **1** shows a very intense absorption spectrum with a molar extinction coefficient as high as 3.39x10^5 in THF at the Soret peak. Also, the weaker Q-bands display respectable molar extinction coefficients in the range of 30000 M^{-1} cm^{-1}. The spectra in toluene display small red shift and some difference in the extinction coefficients.

According to these results, Si-corrole behaves as the higher homologue of Ge-corrole,[14b] where the native Cl-complex quickly hydrolyzed yielding the μ-oxo dimer and the hydroxyl derivatives. We studied the possibility to convert the μ-oxo dimer into the corresponding monomer by reacting a CH$_2$Cl$_2$ solution of complex **2** with concentrated HCl, and then stirring the heterogeneous system for 16 hours. Unexpectedly the UV-vis spectrum of the violet solution collected was very similar to that of the μ-oxo dimer, while the ^{1}H NMR analysis showed many unresolved signals in the aromatic region and many singlets at around 2.7-3.0 ppm, indicating the formation of a more complex structure or of a mixture of products. TLC revealed the presence of two compounds with a very similar R$_f$,
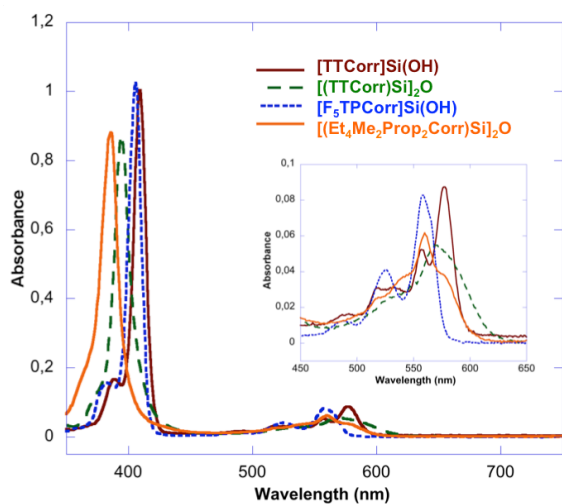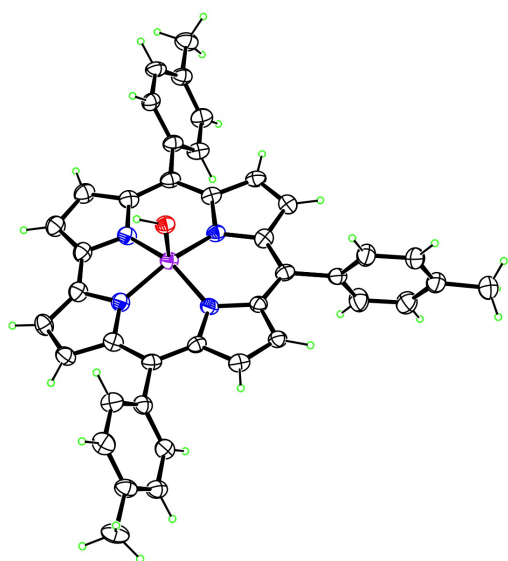
Figure 2. X-ray structure of **1**, one of the two independent molecules, with 50% ellipsoids.

while by mass analysis we observed the peak corresponding to the dimeric form of the silicon corrole, as indicated by the electronic spectrum, functionalized with one or two Cl units. This halogenation could be attributed to the facile oxidation of the corrole ring, which is then halogenated by nucleophilic attack of the chloride ion, and it is similar to that observed in the case of the reaction of chloroauric acid with free base corroles.[18] It is however interesting to note the stability of Si corroles under acidic conditions, which is much higher than for the corresponding porphyrin complexes.[19]

The same synthetic approach allowed the preparation of **3**. The UV-vis spectrum of the complex shows a Soret band at 406 nm and some Q bands in the region 480-570 nm, displaying a lower molar extinction coefficient respect to its non-fluorinated analogue **1** for all absorption bands. In the ^{1}H NMR spectrum a strongly deshielded doublet (9.54 ppm) can be related to the 2/18 protons, as usually occurs for many diamagnetic complexes of $F_5TPCorr$,[20] while the remaining β-pyrrolic protons resonate as doublets between 9.10 and 8.92 ppm. Also, in this case the protons of the inner OH group appear as a broad singlet in the negative region of the spectrum (-4.31 ppm). A different result was obtained from the preparation of the silicon derivative **4**. Similar to what observed with tritolylcorrole, two fractions were collected. The first one, less polar and more abundant, showed a blue-shifted Soret band at 386 nm, while the second fraction has a split Soret band at 398 and 403 nm (Figure S1). This behavior indicates that the first band corresponds to the μ-oxo dimer, and the second to the monomeric form of the silicon-corrole. The μ-oxo dimer **5** unexpectedly features a molar extinction coefficient that is much lower than that expected by doubling that of the monomer.

Luminescence properties. Compounds **1**, **3**, and **5** were characterized by photoluminescence spectroscopy in the visible and NIR (near infrared) regions, at room temperature and at 77 K (Table 1). Corrole **1** displays a very intense emission centered at 586 nm in THF, with a very large quantum yield (0.45 in THF and 0.50 in toluene). It is to note that, especially because of the very high molar absorption coefficient, the overall brightness of **1** is greater than the one of the most common fluorescent dyes, including cyanines, emitting in this spectral region. The excited state lifetime in toluene is 4.8 ns, allowing the unambiguous attribution of this emission to a fluorescence transition. The fast lifetime of **1** is almost doubled in toluene at 77 K, which indicates that the overall quantum yield could reach a very high value, close to unity.

No other emission (phosphorescence) is observed, neither in the visible or in the NIR range, nor at room temperature or at 77 K. The fluorinated corrole **3** features similar photophysical behavior: it displays a structured emission band, blue-shifted by 12 nm, and a similar monoexponential emission decay with lifetime 5.3 ns. Nonetheless, the quantum yield is reduced to almost half compared to **1**. The almost constant lifetime
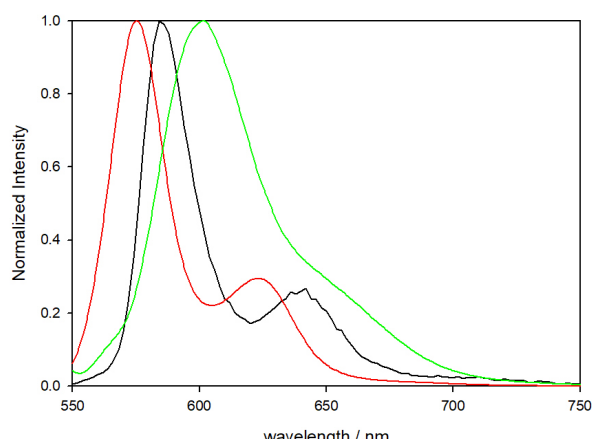

Figure 3. Normalized emission spectra of **1**, **3** and **5** in THF (black, red and green lines, respectively, λ_{exc} = 530 nm).

suggests that the most important variation can be attributed to the radiative constant that decreases upon fluorination of the ligand. The emission spectrum of silicon-alkylcorrole dimers **5**

Table 1. Photophysical properties of **1**, **3** and **5** in THF (and toluene).

	$\varepsilon/M^{-1}cm^{-1}$ (Soret band)	$\varepsilon/ M^{-1}cm^{-1}$ (peak Q-band)	Abs. peak/nm	Quantum yield	Lifetime/ns	Em. peak/nm
1 in THF	339000	31700	409	0.45	5.4	586
1 in toluene	361000	33400	411	0.50	4.8 (8.1 at 77K)	585
3 in THF	266000	23800	407	0.25	5.3	574
5 in THF	298000	22500	386	0.09	4.6	599

is broader and red-shifted. For all the studied compounds, the excitation spectra perfectly match with the absorption spectra both in THF and in toluene, indicating that all bands observed in the absorption spectra lead to the formation of the same emissive excited state.

Finally, only a very small emission of singlet oxygen is observed upon excitation of the corroles, indicating in all cases an inefficient pathway for formation and/or a short lifetime of the triplet state.

Doping of Plus (Pluronica-Silica) NPs. Because of the very high brightness of the corroles **1**, **3**, and **5**, we tested the possibility to embed them inside the silica network of PluS (pluronic shell-silica core) nanoparticles,[21] without previous functionalization of the dyes, in order to obtain structures with even better performances.

In particular, we prepared two samples for each dye, at low and high doping degree respectively, as reported in the SI (Table S1). Interestingly, the nanoparticles are formed and the dyes do not leak during the purification process (dialysis). In addition, the water solutions of nanoparticles are transparent, very concentrated in dye and generally very emissive. These observations suggest that a possible strong interaction takes place between the corroles and the silica, conceivably due to formation of bonds (condensation) of the Si-corroles with the TEOS. A full photophysical characterization was performed, in order to understand the organization, stability and photochemistry of the embedded dyes. Briefly, when using **1** and **3** as doping agents, no aggregation was observed at low doping degree (**NP1L** and **NP3L**). Remarkably, the absorbance (Figure S14) and fluorescence spectra (Figure 4) and the excited state lifetimes of these nanoparticles are very similar to those observed for the respective corrole in THF. On the contrary, in highly doped samples (**NP1H** and **NP3H**) the formation of quenched aggregates leads to a decrease of quantum yield and to a multiexponential lifetime (Table 2). Nonetheless, the molar extinction coefficients of individual NPs are extremely high (exceeding $10^7\,M^{-1}\,cm^{-1}$ in **NP3H**), which ensure that all these synthesized nanoparticles are very bright labels with a high Stokes Shift, when excited at the Soret band. The match between absorbance and excitation spectra reveals also for these nanoparticles that all excited states lead to the formation of the same emissive state (Figure S21 and

S22). Corrole **5** is an exception: the absorbance and emission spectra of **NP5L** and **NP5H** are different from those of **5** in THF, and a multiexponential lifetime is always observed. Furthermore, the excitation spectra at different emission peaks are markedly different. These observations suggest that this dimeric corrole might suffer from chemical reactions with the silanes, leading, most probably, to the breaking of the dimeric structure.

Fluoride detection. Due to the high energy of the Si-F bond (600 kJ/mol) we decided to explore the effectiveness of this
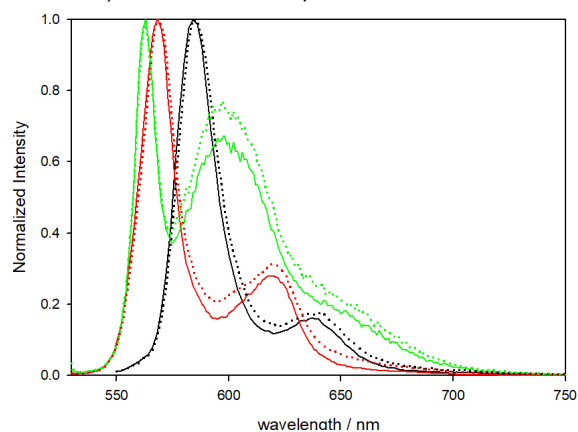
Figure 4. Normalized emission spectra in water of **NP1L**, **NP3L** and **NP5L** (solid black, red and green lines, respectively) and of **NP1H**, **NP3H** and **NP5H** (dotted black, red and green lines, respectively). λexc = 530 nm.

corrole complex as a receptor for F⁻ detection, a species playing an important role in dental care and in the treatment of osteoporosis.[22] Several systems to reveal the presence of fluoride anion have been developed, based on electrochemical, colorimetric or fluorescence methods,[23] with the most common sensing mechanism based on the hydrogen bond formation between N-H and/or O-H subunits and F⁻. The interaction usually amounts to the variation of the chromophore absorbance/emission spectra, which sometime means a color variation that can be seen with the naked-eye. Metal complexes of porphyrins have also been tested as ionophores in potentiometric or optical sensors for fluoride ion detection.[24] However, potentiometric sensors suffered from

Table 2. Photophysical parameters of nanoparticles.

| Sample	ε (NP) / M^{-1} cm^{-1}	Abs. peak / nm	Quantum yield	Lifetime (pre-exponential factor) / ns	Em. Peak / nm
NP1L	1.38×10^6	410	0.13	5.2	586
NP1H	4.26×10^6	410	0.04	1.0 (950) / 4.5 (1500)	586
NP3L	1.89×10^6	406	0.10	5.7	569
NP3H	14.0×10^6	406	0.015	0.9 (500) / 5.5 (2500)	569
NP5L	2.27×10^6	386	0.028	2.7 (1100) / 7.4 (1800)	563 / 598
NP5H	2.55×10^6	386	0.010	2.3 (1200) / 7.1 (1600)	563 / 598

metalloporphyrin dimer formation, while optical devices needed the addition of a pH indicator as a chromoionophore and for this reason, of course, were highly sensitive to solution pH.[25] β-Functionalized Ga corroles have been previously reported to be promising as anion chemosensors showing optical changes when exposed to fluoride ion, although when dispersed in a polymeric matrix they showed quite long response times and they were more efficient for cyanide detection.[24b] Considering the brilliant optical features of Si corroles, we have been interested to determine if the Si-corrole interaction with the F$^-$ ion can occur; a large optical spectrum variation could be obtained, giving a direct fluoride ion detection with large sensitivity and lower detection limit. For this study **1** was chosen as the reference compound, and its affinity toward F$^-$ was measured in organic solvents with differing polarity. A 10^{-6} M solution of **1** in CH_2Cl_2 or DMSO was treated with increasing amounts of a 1 M standard solution of Bu_4NF in THF. A variation of the UV-vis spectrum was observed: the main peak at 413 nm disappeared, being replaced by a split Soret band at 424 and 436 nm, while in the

Q region, the main absorbance at 587 nm was 43 nm red shifted to 630 nm (Figure 5, 6 and S18 and S19).

Upon titration performed with Bu_4NF in CH_2Cl_2 or DMSO, a complete conversion was observed, with the color of the solution turning from pink to green, thereby allowing the easy detection of the chromophore-fluoride interaction in presence of a very small amount of the inorganic anion (experiments were performed in the 4.6×10^{-7}-3×10^{-5} M range). In Figure **7** the corresponding plot for the titration of **1** with Bu_4NF in DMSO is presented. A close analysis reveals a linear change of absorbance maxima (λ_{max} = 411 and 434 nm) of the corrole receptor upon addition of fluoride, with end point at around 1.5 equivalents of guest.

Some elements suggest the formation of a hexa-coordinated complex. First of all, the strong variation observed in the UV-vis spectrum is consistent with a large molecular structure change, such as a coordination number increase, rather than an axial ligand exchange. Indeed, in the Q band region, the UV-vis spectra of the Si-corrole before and after the fluoride treatment closely resemble those of pentacoordinated and hexacoordinated phosphorus complexes,[14a] while the split

Figure 5. UV-vis spectrum of **1** before and after fluoride addition, recorded in DMSO.
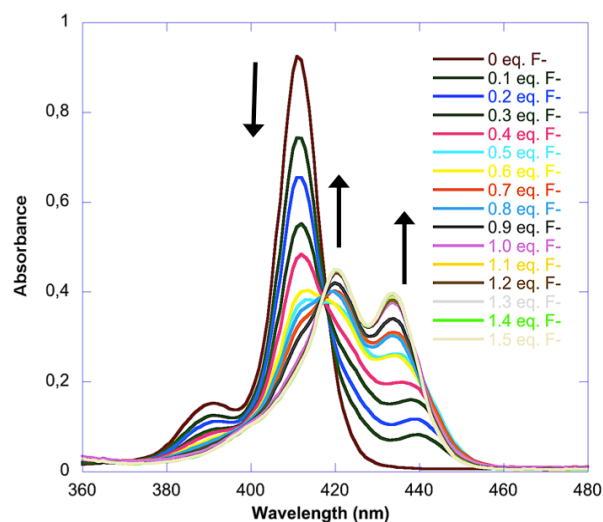
Figure 6. UV-vis spectroscopic titration of **1** with F$^-$ in the Soret region recorded in DMSO.

Soret band suggests a deviation from planarity of the macrocycle.

However, a complex mechanism is present for fluoride binding, which is not the simple coordination of F$^-$ to the free axial position of **1**, but some additional process must occur, as evidenced by the amount of fluoride ion needed and the lack of clear isosbestic point in the titration plot. Interestingly, in these conditions large changes are also observed in the fluorescence spectra, as shown in Figure 8. In particular, an almost complete quenching can be observed below 600 nm, while smaller changes are observed at higher wavelength, so that a ratiometric approach can also be envisaged.

To clarify the **1**-fluoride binding mode, ^{1}H NMR spectroscopy was performed in DMSO-d_6 before and after the Bu$_4$NF addition. The observation of the Si-OH high field signal
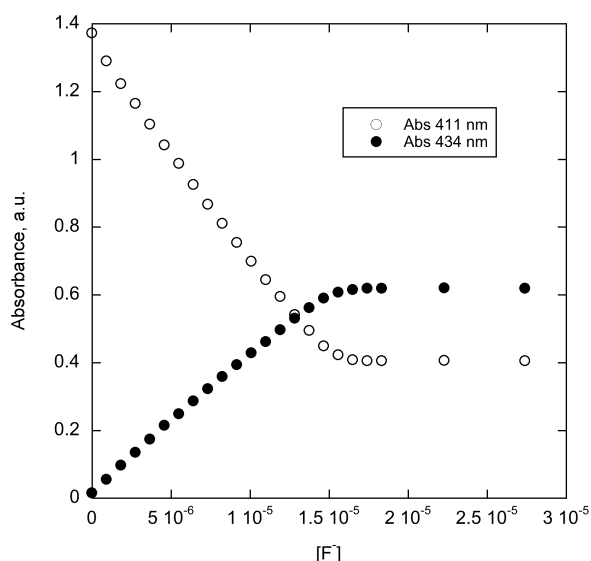

Figure 7. Titration plot of **1** (4.6x10^{-6} n/L) with Bu$_4$NF in DMSO (T = 298 K). Open circles λ = 411 nm; full circles λ = 434 nm.

behavior gave some insights into the processes occurring upon fluoride ion addition.

The initial addition of fluoride ion (up to 0.5 equivalents of F$^-$) induced the appearance of an additional high field resonance at -2.44 ppm, other the initial signal at -0.26 ppm (Figure S6). Further addition of fluoride ion led to the disappearance of this last resonance, with the formation of a novel signal at -6.94 ppm (Figure S6).

This result confirmed the presence of different processes induced by the interaction of **1** with F$^-$. The first process, occurring at low concentration of fluoride ion, led to breaking of the hydrogen bond interaction of the coordinated OH group, with the appearance of the -2.44 ppm signal, and then, with the increased concentration, the fluoride was added to the axial position of the corrole complex leading to the hexacoordinated derivative, characterized by the -6.94 ppm resonance. The hydrogen bond interaction in the starting complex **1** was also confirmed by the concentration dependence of the OH signals in the ^{1}H NMR spectrum of **1** in CDCl$_3$ (Figure S2). The spectrum at 10^{-4} mol/L concentration of **1** shows a signal at -

4.46 ppm of the axial OH group, a chemical shift similar to that observed for the analogous dihydroxy phosphorus corrole complex.[15a] Increasing the concentration of **1** from 10^{-4} to 5x10^{-3} mol/L led to the appearance in the spectrum of a resonance at -1.31 ppm, in addition to the -4.46 ppm resonance of the pristine **1**, due to the formation of a hydrogen bond interaction upon increasing the complex concentration. The changes observed in the high field region of the ^{1}H NMR spectrum were also accompanied by variation of the β-pyrrole chemical shifts, confirming the formation of a new species with respect to the pristine **1** (Figure S5).

Although the binding kinetics are complicated, from the above findings it is possible to assert that Si-corrole **1** is able to detect F$^-$ in solution at very low concentration.

The selectivity toward F$^-$ was studied by comparison of the colorimetric variation induced by other anions. To a 10^{-5} M solution of corrole in DMSO-H$_2$O, an excess of different salts was added, in order to have saturated solutions. Under these conditions fluoride ion induces a color variation after a few seconds, while a small color change was observed after longer time for AcO$^-$ (30 minutes) and NO$_2^-$ (4 hours). Both these solutions are dark violet or blue, making it possible to clearly distinguish them from fluoride, while no variations were induced by the other investigated salts (Figure 9).

To assess the applicability of this chromophore for F$^-$ detection in aqueous systems, a UV-vis spectrophotometric titration was performed with 2 equivalents of NaF in DMSO-H$_2$O solutions of different composition. The spectroscopic pattern of the F$^-$ axially bound to **1** is retained in a DMSO-H$_2$O 80:20% solution, while higher amounts of water lead to corrole aggregation (DMSO < 30%), as indicated by the broadening of the Soret band. These results led us to study the possibility to develop optical sensors based on silicon corrole complexes for the detection of fluoride. To make the system suitable for application to real situations, the response due to the analyte interaction should be as clear and quick as possible; much more, a low-cost device could guarantee a large scale application. To reach this target, we decided to investigate two different strategies, the first one based on the photophysical properties of the silica nanoparticles. We have thus prepared micromolar nanoparticle solutions of **NP1L**, and we have added increasing amounts of a concentrated NaF solution in
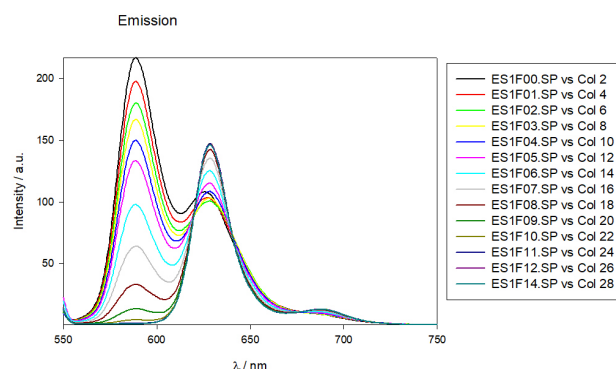

Figure 8. Fluorescence spectra (λ_{exc} = 530 nm) of **1** in DMSO and upon addition of increasing amounts of F$^-$.

water. These nanoparticles showed, just after the addition, only a small change in their photophysical properties. We measured again the fluorescence after 2 days, observing a substantial change in the absorption spectrum and an almost complete quenching of fluorescence of both samples. Further experiments are ongoing to investigate the nature of the significant fluorescence quenching observed; it is however clear that this approach cannot lead, at least under these conditions, to the design of an effective device.

Figure 9. Colorimetric variation of **1** in presence of different anions; L correspond to the pristine solution of **1**.

Another approach was instead based on the dispersion of **1** into a polymeric membrane, usually exploited to develop optical and potentiometric sensors,[23a] where the corrole derivative acts as an ionophore. Considering the previously hypothesized working mechanism of the receptor, two different kinds of membrane were made, with **1** as ionophore and with or without an ionic exchanger (tetradodecylammonium chloride, TDAC). Polymeric membranes were deposited on a glass surface and dipped into a water solution containing 10^{-3} M of Bu_4NF or NaF, to further verify the sensing mechanism. The membrane with no TDAC showed no response toward NaF and a weak color change in the solution of Bu_4NF, due to the lipophilicity of the organic cation, which ensures low solubility of the salt in the polymeric material. The TDAC doped membrane has a more rapid response to F^-, changing color from pink to green, regardless to the cation nature, thus confirming the formation of the hexacoordinated anionic fluoride complex of **1**. If F^- replaces OH^-, the ionophore remains a neutral molecule, so it should be independent of the presence of the ionic exchanger, while if Si-corrole binds fluoride and hydroxide, the resulting anionic complex should react quickly in presence of the TDAC. We then decided to test the membrane selectivity and sensitivity. The first parameter was examined repeating the measurements with a series of different anions: F^-, Cl^-, Br^- I^-, NO_2^-, NO_3^-, AcO^-, H_2PO_4; we compared membranes with 0, 0.5, 1 and 2 equivalents of ionic exchanger respectively. After 20 minutes all the membranes in contact with the Bu_4NF solution became green, while in the case of the inorganic salts the addition of TDAC to the membrane was essential to have a color variation. In this case a partial color change was also seen with AcO^- and NO_2^- ions, for the membranes containing 2 equivalents of TDAC, while a strong green coloration was observed for F^- (NaF source, membranes with 1 or 2 equivalents of TDAC). Because the

interfering anions were also weak bases, we decided to study the influence of solution pH on the membrane responses. We repeated the same experiments in different buffers, at pH = 5.5 and pH = 8.8. At pH = 8.8 the membranes changed the color from red to green upon addition of the ions; at pH = 5.5 the color change was registered only in the case of F^-, while both AcO^- and NO_2^- were not effective. It should also be noted that the color change was not the same for these ions, showing a more brilliant green in the case of F^-. This result seems to indicate that OH^- is probably the interfering ion. For this reason, we added a diluted NaOH solution to **1** in DMSO, observing also in this case changes in the UV-vis spectrum, with the Soret band splitting and a red shift of both Soret and Q bands larger than those observed in the case of fluoride ion (Figure S20). We can deduce that OH^- is able to form a hexacoordinated species similar to that formed by F^-. However, when we consider the potential real-world applications, the pH of the samples can be controlled, so minimizing this potential problem.

Although these results confirmed the potential of **1** as a fluoride ion receptor, the optode response times were also in this case not satisfying. Recently, an interesting article related to the exploitation of a paper-based membrane-free optical device, based on an aluminum porphyrin complex has been reported in the literature.[26] We have been interested in this approach because on one hand the possibility to avoid the use of a polymeric membrane could greatly reduce the sensor response time and, on the other hand, it can allow the realization of inexpensive disposable devices for fluoride detection. Different spots of a **1** and TDAC mixture (1:1 equivalents) from a THF solution were deposited on Whatman Grade 42 ashless filter paper strips by drop casting. When the paper strip was immersed in a water solution of NaF, buffered at pH = 5.5, the spot immediately changed in color from pink red to olive green. In the absence of TDAC, the color change of the spot required a longer time (about 10 minutes). The sensitivity of the developed optode was quite high and it was possible to observe the color change with the naked eye up to a 10^{-5} mol/L solution of NaF (Figure 10). We studied the selectivity of the optode with respect to the same series of anions previously tested; also in this case in solutions were buffered at pH = 5.5. No color changes were observed, confirming in this case the optode selectivity towards the fluoride ion.

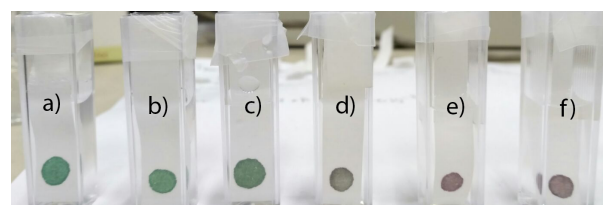**Figure 10.** Paper strips color variations upon exposure to fluoride solutions in MES buffer (pH = 5.5): a) 10^{-2} mol/L, b) 10^{-3} mol/L, c) 10^{-4} mol/L, d) 10^{-5} mol/L, e) 10^{-6} mol/L, f) blank.

Conclusions

The preparation of the Si derivative of corrole adds a further component to the "periodic table" of metallocorrolates.[27] The peripheral substituents of the corrole ring strongly influence the nature of the metalation products. With β-alkyl corroles, a μ-oxo dimer is the main product, while a hydroxo-complex is obtained when electron withdrawing substituents are present, such as in the case of 5,10,15-tris-(pentafluorophenyl)corrole. All attempts to convert the μ-oxo dimer into the corresponding monomer failed, demonstrating on the high stability of the Si corrole complex towards in acidic conditions. Si corrole complexes display very good photophysical properties, with intense fluorescence emission characterized by high quantum yields. These optical features are maintained when monomeric complexes **1** and **3** were embedded in Si nanoparticles. The optical properties of **1** were significantly influenced in the presence of fluoride ions, which induced significant changes in both absorption and fluorescence spectra. For these reasons, **1** is particularly appealing for the design of highly efficient optical sensors for fluoride detection. In view of this, we have first studied the selectivity of **1** towards fluoride binding in a DMSO/H$_2$O mixture. The good results obtained led us to investigate the suitability of **1** as chromoionophore so as to develop optical sensors for the F$^-$ ion. While both functionalized Si nanoparticles and polymeric membranes showed some important drawbacks for their applications, the exploitation of paper based optode gave satisfying results, which makes these species promising for application in the real field.

Experimental Section

General procedures. Reagents and solvents (Sigma-Aldrich, Fluka, Merck, and Carlo Erba) were of synthetic grade and were used without further purification. Silica gel 60 (70−230 mesh) or neutral alumina (Brockmann grade III) was used for chromatography. UV−visible spectra were measured in CH$_2$Cl$_2$ or DMSO with a Varian Cary 50 spectrophotometer or a Hewlett-Packard model 8453 diode-array spectrophotometer. ^{1}H and ^{19}F spectra were recorded at 300 K with a Bruker Avance III 400 BBFO spectrometer operating at 400.13 MHz for ^{1}H and 376.50 MHz for ^{19}F equipped with a 5 mm inverse broadband probe. All experiments were performed in CDCl$_3$ or DMSO-d_6. Chemical shifts are given in ppm relative to residual solvents (CHCl3 = 7.26 ppm, DMSO = 2.50 ppm).

Synthesis. 5,10,15-Tritolylcorrole (TTCorrH$_3$),[6a] 5,10,15-Tris(2,3,4,5,6-pentafluorophenyl)corrole (F$_5$TPCorrH$_3$),[25] and AlkCorrH$_3$[3] were prepared following literature methods.

(Hydroxy)[5,10,15-tritolylcorrolato]silicon [TTCorr]Si(OH). TTCorrH$_3$ (60 mg, 0.106 mmol) was dissolved in 20 ml of anhydrous pyridine and mixture heated under nitrogen. Si$_2$Cl$_6$ (547 μL, 3.18 mmol, 30 eq.) was added under inert atmosphere and the mixture was further stirred under reflux for 1 hour. The solution becomes dark green then pink. Once the complex formation was verified by UV-vis spectroscopy, the mixture was left to cool then quenched by careful addition of water. The residue was filtered on paper to remove the silica formed and immediately dissolved with a 1:1 methanol/THF mixture. Solvent was

removed and the residue purified by column chromatography on Al$_2$O$_3$ eluted with CH$_2$Cl$_2$ to collect the μ-oxo dimer, then with CHCl$_3$ for the [TTCorr]Si(OH).

[(5,10,15-Tritolylcorrolato)silicon]μ-oxo dimer [(TTCorr)Si]$_2$O. Crystallized from CH$_2$Cl$_2$/pentane. Yield: 8 mg (6%). Mp: >300 °C. UV−vis [CH$_2$Cl$_2$; λ$_{max}$, nm (log ε, M^{-1} cm^{-1})]: 394 (4.80), 525 (3.22), 566 (3.51), 586 (sh). ^{1}H NMR (400.13 MHz, CDCl$_3$): δ 8.78 (br s, 4 H, β-pyrrole), 8.56 (br s, 6 H, β-pyrrole), 8.32 (br s, 6 H, β-pyrrole), 8.21 (br s, 2 H, meso-phenyl), 7.70 (br s, 6 H, meso-phenyl), 7.51-7.36 (m, 14 H, meso-phenyl), 2.76 (br s, 12 H, phenyl-CH$_3$), 2.70 (br s, 6 H, phenyl-CH3). MS (FAB): m/z 1203 [M$^+$] (100%). Elem anal. Calcd for C$_{80}$H$_{58}$N$_8$OSi$_2$: C, 79.84; H, 4.86; N, 9.31. Found: C, 79.78; H, 4.81; N, 9.38.

(Hydroxy)[5,10,15-tritolylcorrolato]silicon [TTCorr]Si(OH). Crystallized from CH$_2$Cl$_2$/methanol. Yield: 45 mg (70 %). Mp: >300 °C. UV−vis [CH$_2$Cl$_2$; λ$_{max}$, nm (log ε, M^{-1} cm^{-1})]: 389 (4.75), 409 (5.54), 519 (4.00), 532 (4.01), 559 (4.30), 578 (4.52). ^{1}H NMR (400.13 MHz, CDCl$_3$): δ 9.36 (d, 2 H, J = 4.26 Hz, β-pyrrole), 9.20 (d, 2 H, J = 4.87 Hz, β-pyrrole), 9.07 (d, 2 H, J = 4.29, Hz, β-pyrrole), 8.90 (d, 2 H, J = 4.88, Hz, β-pyrrole), 8.18 (unresolved multiplet, 5 H, meso-phenyl), 7.92 (d, 1 H, J = 7.63 Hz, meso-phenyl), 7.61 (m, 5 H, meso-phenyl), 7.54 (d, 1 H, J = 7.69 Hz, meso-phenyl), 2.70 (s, 6 H, phenyl-CH$_3$), 2.69 (s, 3 H, phenyl-CH$_3$), -4.46 (br s, 1 H, Si-OH). MS (FAB): m/z 747 [M-OH+nitrobenzil alcohol] (100%). Elem anal. Calcd for C$_{40}$H$_{30}$N$_4$OSi: C, 78.66; H, 4.95; N, 9.17. Found: C, 78.74; H, 4.98; N, 9.12.

(Hydroxy)[Tris(2,3,4,5,6-pentafluorophenyl)corrolato]silicon [F$_5$TPCorr]Si(OH). F$_5$TPCorrH$_3$ (60 mg, 0.075 mmol) was dissolved in 20 ml of anhydrous pyridine and the mixture was heated under nitrogen. Si$_2$Cl$_6$ (387 μL, 2.25 mmol, 30 eq.) was added under an inert atmosphere and the mixture was further stirred under reflux for 1 hour. The solution becomes dark green then pink. Once the complex formation was verified by UV-vis spectroscopy, the mixture was left to cool then quenched by careful addition of water. The residue was filtered on paper to remove the silica formed and then dissolved with a 1:1 methanol/THF mixture. The solvent was removed and the residue was purified by column chromatography on Al$_2$O$_3$ eluted with CHCl$_3$/hexane 1:1 to collect the [F$_5$TPCorr]Si(OH), crystallized from CH$_2$Cl$_2$/pentane. Yield: 36 mg (58 %). Mp: >300 °C. UV−vis [CH$_2$Cl$_2$; λ$_{max}$, nm (log ε, M^{-1} cm^{-1})]: 384 (4.71), 406 (5.49), 489 (3.61), 525 (4.13), 559 (4.43). ^{1}H NMR (400.13 MHz, CDCl$_3$): δ 9.54 (d, 2 H, J = 4.39 Hz, β-pyrrole), 9.10 (d, 2 H, J = 4.81 Hz, β-pyrrole), 9.07 (d, 2 H, J = 4.33, Hz, β-pyrrole), 8.92 (d, 2 H, J = 4.83, Hz, β-pyrrole), -4.31 (br s, 1 H, Si-OH). ^{19}F NMR (376.50 MHz, DMSO-d_6) δ -138.63 (dd, ^{3}J (F,F) = 25.04 Hz, ^{4}J (F,F) = 6.74 Hz, 2 F, o-F, Ph-5,15), -138.97 (dd, ^{3}J (F,F) = 25.86 Hz, ^{4}J (F,F) = 7.58 Hz, 1 F, o-F, Ph-10), -139.08 (dd, ^{3}J (F,F) = 25.52 Hz, ^{4}J (F,F) = 6.32 Hz, 2 F, o-F, Ph-5,15), -139.39 (dd, ^{3}J (F,F) = 25.75 Hz, ^{4}J (F,F) = 6.32 Hz, 1 F, o-F, Ph-10), -154.55 (t, ^{3}J (F,F) = 22.37 Hz, 2 F, p-F, Ph-5,15), -154.75 (t, ^{3}J (F,F) = 22.50 Hz, 1 F, p-F, Ph-10), -162.49/-162.89 (m, 6 F, m-F). MS (FAB): m/z 976 [M-OH+nitrobenzil alcohol] (100%). Elem anal. Calcd for C$_{37}$H$_9$F$_{15}$N$_4$OSi: C, 53.00; H, 1.08; N, 6.68. Found: C, 53.02; H, 1.10; N, 6.59.

(Hydroxy)[(2,3,17,18-tetraethyl-7,13-dimethyl-8,12-dimethoxycarbonylpropyl)corrolato]silicon [Et$_4$Me$_2$Prop$_2$Corr]Si(OH). AlkCorrH$_3$ (70 mg, 0.121 mmol) was dissolved in 20 ml of anhydrous pyridine and the mixture was heated under nitrogen. Si$_2$Cl$_6$ (626 μL, 3.63 mmol, 30 eq.) was added under an inert atmosphere and the mixture was further stirred under reflux for 1 hour. The solution becomes dark green then pink. Once complex formation was verified by UV-vis spectroscopy, the mixture was left to cool then quenched by careful addition of water. The residue was

filtered on paper to remove the silica formed and then dissolved in a 1:1 methanol/THF mixture. The solvent was removed and the residue was purified by column chromatography on Al_2O_3 eluted with CH_2Cl_2 and then with $CHCl_3$ to collect two fractions; the first fraction corresponded to the μ-oxo dimer and the second to the monomeric form of silicon corrole.

[(2,3,17,18-Tetraethyl-7,13-dimethyl-8,12-dimethoxycarbonylpropylcorrolato)silicon] μ-oxo dimer [(Et₄Me₂Prop₂Corr)Si]₂O. Crystallized from CH_2Cl_2/pentane. Yield: 40 mg (26 %). Mp: >300 °C. UV−vis [CH_2Cl_2; λ$_{max}$, nm (log ε, M^{-1} cm^{-1})]: 386 (5.60), 519 (4.03), 560 (4.43), 576 (4.24). ¹H NMR (400.13 MHz, DMSO-d_6): δ 8.74 (s, 2 H, 10 *meso*-H), 8.72 (s, 4 H, 5,15 *meso*-H), 4.46-4.39 (m, 4H, β-$CH_2CH_2CO_2CH_3$), 4.26-4.18 (m, 4H, β-$CH_2CH_2CO_2CH_3$), 3.85-3.71 (m, 16 H, β-$CH_2CH_2CO_2CH_3$ + β-CH_2CH_3), 3.53 (s, 12 H, β-$CH_2CH_2CO_2CH_3$), 3.46 (s, 12 H, β-CH_3), 3.07-2.96 (m, 8 H, β-CH_2CH_3), 1.73 (t, 12 H, *J* = 7.59 Hz, β-CH_2CH_3), 1.62 (t, 12 H, *J* = 7.61 Hz, β-CH_2CH_3). MS (FAB): m/z 1286 [M+] (100%). Elem anal. Calcd for $C_{74}H_{86}N_8O_9Si_2$: C, 69.02; H, 6.73; N, 8.70. Found: C, 69.09; H, 6.80; N, 8.61.

(Hydroxy)[(2,3,17,18-tetraethyl-7,13-dimethyl-8,12-dimethoxycarbonylpropyl)corrolato]silicon [Et₄Me₂Prop₂Corr]Si(OH). Crystallized from CH_2Cl_2/pentane. Yield: 4 mg (5 %). Mp: >300 °C. UV−vis [CH_2Cl_2; λ$_{max}$, nm (log ε, M^{-1} cm^{-1})]: 371 (4.46), 388 (4.72), 398 (5.08), 403 (5.05), 485 (3.38), 522 (3.82), 559 (4.26). ¹H NMR (400.13 MHz, $CDCl_3$): δ 9.86 (s, 2 H, 5,15 *meso*-H), 9.82 (s, 1 H, 10 *meso*-H), 4.48-4.34 (m, 8 H, β-$CH_2CH_2CO_2CH_3$), 4.26-4.19 (m, 8 H, β-CH_2CH_3), 3.69 (s, 6 H, β-$CH_2CH_2CO_2CH_3$), 3.65 (s, 6 H, β-CH_3), 1.93 (t, 6 H, *J* = 7.60 Hz, β-CH_2CH_3), 1.86 (t, 6 H, *J* = 7.60 Hz, β-CH_2CH_3), -4.96 (br s, 1 H, Si-OH). MS (FAB): m/z 788 [M-OH+2-nitrobenzyl alcohol)] (50%). Elem anal. Calcd for $C_{37}H_{44}N_4O_5Si$: C, 68.07; H, 6.79; N, 8.58. Found: C, 68.11; H, 6.84; N, 8.51.

Membranes preparation. A polymeric membrane of 100 mg weight was prepared dissolving 1 mg of [TTCorr]Si(OH), 33 mg of PVC and 66 mg (72 μL) of DOS (bis(2-ethylhexyl) sebacate) in 1 mL of anhydrous THF; the given amount of ionic exchanger (Tetradodecylammonium Chloride) was added if needed. Mixture was, vigorously stirred for 5 minutes then let to completely dissolved overnight and finally cast onto a transparent glass slide

Crystallography. The crystal structure of 1 as the hemi-benzene solvate was determined using low-temperature (90K) data from a Bruker Kappa APEX-II DUO diffractometer with CuKα radiation. There are two independent molecules of the Si complex and one benzene solvent molecule. One Si complex has its SiOH group disordered on either side of the corrole plane with 0.577:0.423 populations. H atoms were located from difference maps but constrained in calculated positions during refinement, except for the OH hydrogen atom of the the disordered molecule, which was not located. Crystal data: $C_{40}H_{30}N_4OSi$. ½ C_6H_6, M = 649.82, red-orange plate, triclinic, a = 9.7911(5), b = 13.1955(7), c = 26.2467(14) Å, α = 92.857(4), β = 100.489(4), γ = 102.126(4)°, U = 3246.3(3) Å3, T = 90 K, space group P-1, Z = 4, Dc = 1.330 g cm-3, μ(CuKα) = 0.97 mm-1, 20307 reflections measured, θmax = 61.2˚, 9652 unique (Rint = 0.051). The final R = 0.094 (7664 I>2σ(I) data), wR(F2) = 0.260 (all data), GOF = 1.11, 902 parameters, CCDC 1572820.

Acknowledgements

[1] D. A. W. Johnson, I. T. Kay, *J. Chem. Soc.* **1965**, 1620-1629.
[2] a) R. Paolesse, L. Jaquinod, D. J. Nurco, S. Mini, F. Sagone, T. Boschi, K. M. Smith, *Chem. Commun.* **1999**, 1307-1308. (b) Z. Gross, N. Galili, I. Saltsman, *Angew. Chem. Int. Ed.* **1999**, *38*, 1427-1429.
[3] R. Paolesse in *The Porphyrin Handbook, Vol. 2 (*Eds.: K. M. Kadish, K. M. Smith, R. Guilard), Academic Press, San Diego, **2000,** pp 201−232.
[4] a) A. Ghosh, T. Wondimagegn, A. B. J. Parusel, *J. Am. Chem. Soc.* **2000**, *122*, 5100-5104. b) F. A. Walker, S. Licoccia, R. Paolesse, *J. Inorg. Biochem.* **2006**, *100*, 810-837. c) A. Ghosh, *Chem. Rev.* **2017**, *117*, 3798-3881.
[5] a) S. Bose, A. Pariyar, A. N. Biswas, P. Das, P. Bandyopadhyay, *Catal. Commun.* **2011**, *12*, 1193−1197. (b) C. M. Lemon, D. K. Dogutan, D. G. Nocera in *Handbook of Porphyrin Science, Vol. 21 (*Eds.: K. M. Kadish, K. M. Smith, R. Guilard), World Scientific Publishing, Singapore, **2012**, pp 1−143 c) J. Jung, S. Liu, K Ohkubo, M. M. Abu-Omar, S. Fukuzumi, *Inorg. Chem.* **2015**, *54*, 4285−4291. d) H. Lei, H. Fang, Y. Han, W. Lai, X. Fu, R. Cao, *ACS Catal.* **2015**, *5*, 5145–5153.
[6] a) R. Paolesse, A. Marini, S. Nardis, A. Froiio, F. Mandoj, D. J. Nurco, L. Prodi, M. Montalti, K. M. Smith, *J. Porphyrins Phthalocyanines* **2003**, *7,* 25-36 b) T. Ding, E. A. Alemán, D. A. Modarelli, C. J. Ziegler, *J. Phys. Chem. A* **2005**, *109*, 7411-7417. c) B. Ventura, A. Degli Esposti, B. Koszarna, D. T. Gryko, L. Flamigni, *New J. Chem.* **2005**, *29*, 1559-1566.
[7] L. Flamigni, D. T. Gryko, *Chem. Soc. Rev.* **2009**, *38*, 1635-1646.
[8] D. Samaroo, E. Perez A. Aggarwal, A. Wills, N. O'Connor, *Ther. Delivery.* **2014**, *5*, 859-872.
[9] R. Paolesse, S. Nardis, D. Monti, M. Stefanelli, C. Di Natale, *Chem. Rev.* **2017**, *117*, 2517-2583.
[10] M. Gouterman, in *The Porphyrins, Vol. III (*Ed.: D. Dolphin), Academic Press, New York, **1979**, pp 1−165.
[11] a) A. M. Albrett, J. Conradie, P. D. W. Boyd, G. R. Clark, A. Ghosh, P. J. Brothers, *Am. Chem. Soc.* **2008**, *130*, 2888-2889. b) A. M. Albrett, K. E. Thomas, S. Maslek, A. Młodzianowska, J. Conradie, C. M. Beavers, A. Ghosh, P. J. Brothers, *Inorg. Chem.* **2014**, *53*, 5486-5493.
[12] a) A. Mahammed, Z. Gross, *J. Inorg. Biochem.* **2002**, *88*, 305-309. b) X. Liu, A. Mahammed, U Tripathy, Z. Gross, R. P. Steer, *Chem. Phys. Lett.* **2008**, *459*, 113-118. c) D. Kowalska, X. Liu, U. Tripathy, A. Mahammed, Z. Gross, S. Hirayama, R. P Steer, *Inorg. Chem.* **2009**, *48*, 2670-2676.
[13] J. Bendix, I. J. Dmochowski, H. B. Gray, A. Mahammed, L. Simkhovich Z. Gross, *Angew. Chem. Int. Ed.* **2000**, *39*, 4048-4051.
[14] a) L. Simkhovich, A. Mahammed, I. Goldberg, Z. Gross, *Chem. Eur. J.* **2001**, *7*, 1041-1055. b) S. Nardis, F. Mandoj, R. Paolesse, F. R. Fronczek, K. M. Smith, L. Prodi, M. Montalti G. Battistini, *Eur. J. Inorg. Chem.* **2007**, 2345-2352.
[15] a) A. Ghosh, M. Ravikanth, *Chem. Eur. J.* **2012**, *18*, 6386-6396. b) A. Ghosh, W.-Z. Lee, M. Ravikanth, *Eur. J. Inorg. Chem.* **2012**, 4231-4239. c) X. Liang, J. Mack, L.-M. Zheng, Z. Shen, N. Kobayashi, *Inorg. Chem.* **2014**, *53*, 2797-2802. d) J. Vesfrid, R. Kothari, A. Kostenko, I. Goldberg, B. Tumanskii, Z. Gross, *Inorg. Chem.* **2016**, *55*, 6061-6067.
[16] J. F. B. Barata, M. G. P. M. S. Neves, M. A. F. Faustino, A. C. Tomé, J. A. S. Cavaleiro, *Chem. Rev.* **2017**, *117*, 3192-3253.
[17] X. F. Zhang, Y. Rong, *J. Photochem. Photobiol. A: Chem.* **2011**, *222*, 141-145.

[18] K. E. Thomas, A. A. Alemayehu, J. Conradie, C. Beavers, A. Ghosh, *Inorg. Chem.* **2011***, 50,* 12844−12851.

[19] a) K. M. Kane, F. R. Lemke, *Inorg. Chem.* **1995**, *34*, 4085-4091. b) K. M. Kane, C. R. Lorenza, D. M. Heilman, F. R. Lemke, *Inorg. Chem.* **1998**, *37*, 669-673. c) S. N. Remello, F. Kuttassery, T. Hirano, Y. Nabetani, D. Yamamoto, S. Onuki, H. Tachibana H. Inoue, *Dalton Trans.* **2015**, *44*, 20011-20020.

[20] Y. S. Balazs, I. Saltsman, A. Mahammed, E. Tkachenko, G. Golubkov, J. Levine, Z. Gross, *Magn. Reson. Chem.* **2004**, *42*, 624-635.

[21] a) S. Ayoob, A. K. Gubta, *Crit. Rev. Environ. Sci. Technol.* **2006**, *36*, 433-487. b) M. Kleerekoper, *Endocrinol. Metab. Clin. North Am.* **1998**, *27*, 441-452.

[22] a) Y. Zhou, J. F. Zhang, J. Yoon, *Chem. Rev.* **2014**, *114*, 5511-5571 and references herein. b) H. Khanmohammadi, K. Rezaeian, *RSC Adv.* **2014**, *4*, 1032-1038.

[23] a) L. Lvova, C. Di Natale, R. Paolesse, *Sens. Actuators, B.* **2013**, *179*, 21-31. b) C. I. M. Santos, E. Oliveira, J. F. B. Barata, M. A. F. Faustino, J. A. S. Cavaleiro, M. G. P. M. S. Neves, C. Lodeiro, *J. Mater Chem.* **2012**, *22*, 13811-13819.

[24] M. Montalti, L. Prodi, E. Rampazzo, N. Zaccheroni, *Chem. Soc. Rev.* **2014**, *43*, 4234-4268.

[25] D. T. Gryko, B. Koszarna, *Org. Biomol. Chem.* **2003**, *1*, 350-357.

[26] X. Wang, Q. Zhang, C. Nam, M. Hickner, M. Mahoney, M. E. Meyerhoff, *Angew. Chem. Int. Ed.* **2017**, *56*, 11826-11830.

[27] After the present paper had been submitted and reviewed, a report of the synthesis of monomeric Si(IV) complexes of triarylcorroles from the reaction of $SiCl_4$ and corrole in 1,2 dichloroethane appeared in this journal: K. Ueta, M. Fukuda, G. Kim, S. Shimizu, T. Tanaka, D. Kim, A. Osuka, *Chem. Eur. J.* **2018**, Early View, doi: 10.1002/chem.201800165.

Entry for the Table of Contents

FULL PAPER

Have an eye for fluoride ion: The binding of fluoride ion to the newly synthesized Si(IV) corrole complexes induces a color change that can allow to develop paper strips able to allow a naked eye detection of fluoride ions in water samples.
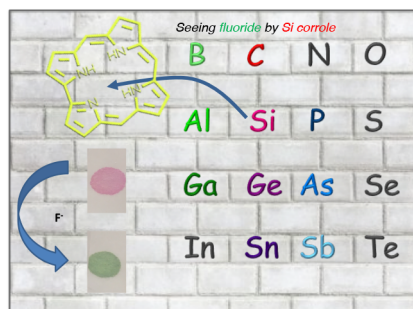
Giuseppe Pomarico, Donato Monti, Martina Bischetti, Andrea Savoldelli, Frank R. Fronczek, Kevin M. Smith, Damiano Genovese, Luca Prodi and Roberto Paolesse*

Page No. – Page No.

Another brick in the wall of metallo-corrolates: Silicon (IV) corroles